Biosensors and Bioelectronics 98 (2017) 428–436

Contents lists available at ScienceDirect

Biosensors and Bioelectronics

journal homepage: www.elsevier.com/locate/bios

Autonomous electrochemical biosensors: A new vision to direct methanol fuel cells

M. Goreti F. Sales, Lúcia Brandão*

BioMark/CINTESIS, Instituto Superior de Engenharia do Porto (ISEP), R. Dr. António Bernardino de Almeida, 431, 4249-015 Porto, Portugal

ARTICLE INFO

Keywords:
User-friendly biosensor
Triple-phase boundary layer
DMFC transducer
Plastic antibody

ABSTRACT

A new approach to biosensing devices is demonstrated aiming an easier and simpler application in routine health care systems. Our methodology considered a new concept for the biosensor transducing event that allows to obtain, simultaneously, an equipment-free, user-friendly, cheap electrical biosensor. The use of the anode triple-phase boundary (TPB) layer of a passive direct methanol fuel cell (DMFC) as biosensor transducer is herein proposed. For that, the ionomer present in the anode catalytic layer of the DMFC is partially replaced by an ionomer with molecular recognition capability working as the biorecognition element of the biosensor. In this approach, fuel cell anode catalysts are modified with a molecularly imprinted polymer (plastic antibody) capable of protein recognition (ferritin is used as model protein), inserted in a suitable membrane electrode assembly (MEA) and tested, as initial proof-of-concept, in a non-passive fuel cell operation environment. The anchoring of the ionomer-based plastic antibody on the catalyst surface follows a simple one-step *grafting from* approach through radical polymerization. Such modification increases fuel cell performance due to the proton conductivity and macroporosity characteristics of the polymer on the TPB. Finally, the response and selectivity of the bioreceptor inside the fuel cell showed a clear and selective signal from the biosensor. Moreover, such pioneering transducing approach allowed amplification of the electrochemical response and increased biosensor sensitivity by 2 orders of magnitude when compared to a 3-electrodes configuration system.

1. Introduction

Incredibly low detection limits can be achieved with electrical biosensors (Cardoso et al., 2016; Sadik et al., 2009) mainly using powerful techniques, such as electrochemical impedance spectroscopy and voltammetric analysis. However their generalized use in routine healthcare systems, in Point-of-Care, or at home for screening relevant markers present at very low levels in the human body may become limited. This is due to the need of both relevant electrical equipment and technical personnel for the analysis and interpretation of the signal. In this work, an innovative approach is proposed to solve such limitations by inserting the biorecognition layer into a highly efficient abiotic fuel cell (a direct methanol fuel cell - DMFC) working as the transducer of the biosensor.

Scheme 1 shows a graphic representation of the new sensory platform. Fuel cell anode catalysts are modified with a selective molecularly imprinted polymer (MIP) and inserted in a membrane electrode assembly (MEA) (step 1). In its turn, this MEA is suitably assembled in a proper holding device (step 2), appropriate for passive direct methanol fuel cell (DMFC) operation. Regarding utilization of the proposed device, a fluid sample (few drops) from a patient is incubated at biosensor's surface (in this case, at the anode side of the fuel cell) (step 3); after washing of the fluid sample, few drops of the fuel (methanol aqueous solution) is added to the anode of the fuel cell (step 4) while oxygen from air (passive operation), at the cathode, will be capable of changing the colour or illuminate a compactly integrated DC powered signalling device. Such user-friendly platform can be used at the health-care provider's office, at home or in Point-of-Care. In there, the device will indicate the presence or not of a certain protein (e.g. related to cancer, tuberculosis, etc.) marker in the sample analysed, signalling a biomarker related to a possible disease or condition.

The biorecognition layer in the proposed biosensor is based on molecular imprinting (Sadeghi et al., 2014; Schirhagl, 2014), particularly surface imprinting. This approach is suitable for the imprinting of voluminous molecules, such as proteins, once the imprinted binding sites are located at the surface of a base material (in this case the catalyst). This hinders the difficulty (due to mass transport limitations) that arises when large biomolecules need to access the binding sites within the 3D structure of the polymer (Mathur et al., 2013; Viswanathan et al., 2012; Zahedi et al., 2016).

* Corresponding author.
E-mail address: lrb@isep.ipp.pt (L. Brandão).

http://dx.doi.org/10.1016/j.bios.2017.07.021
Received 19 April 2017; Received in revised form 28 June 2017; Accepted 8 July 2017
Available online 11 July 2017

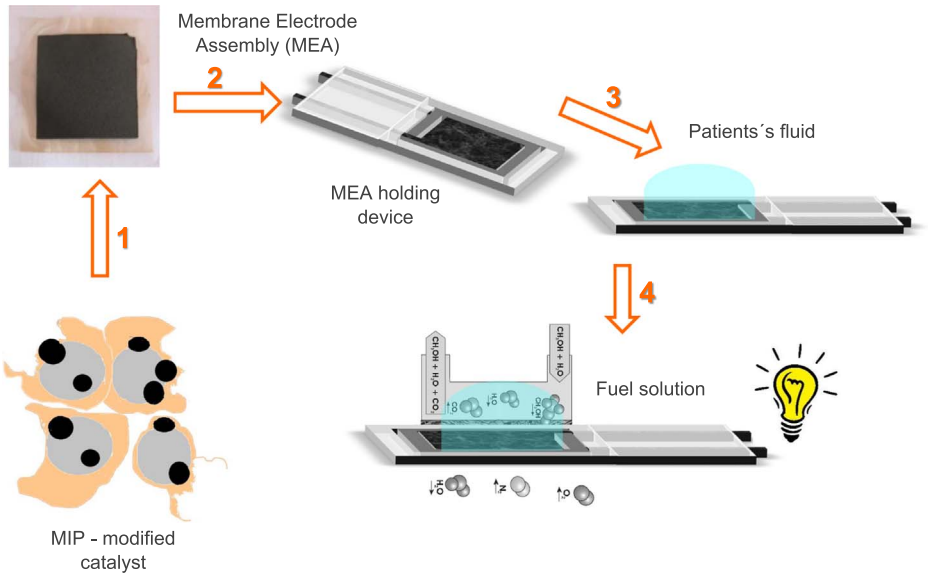

Scheme 1. Graphic representation of the electrically autonomous sensory platform.

The basic principle of the herein proposed biosensor is that upon binding, the biomarker adsorbs to the imprinted selective cavity on the MIP layer and the fuel cell anode catalyst underneath is affected by the protein presence causing a change on the electrochemical oxidation of methanol. This will affect DMFC power performance. The biosensor will be completely autonomous (fully passive fuel cell operation), very small, and disposable due to the low cost (human resources and equipment are usually the most expensive ones). By being highly cost effective, this innovative approach may allow e.g. health-related screening tests everywhere, even in low and middle income countries.

Electrochemical biosensors have been indeed recently transduced by fuel cells but so far only microbial (Asghary et al., 2016; Kim et al., 2007) or enzymatic (Han et al., 2015; Moreira et al., 2017) fuel cells have been applied. These applications use bacteria, enzymes or DNA for biorecognition and appropriate extra care must be given due to cell death or enzyme deactivation. Moreover, such types of fuel cell still present low power performances thus hindering its real application in any current practical system considering small devices. However, these stand-alone applications point to a quite big market need for Point-of-Care applications and following the recent trend on biosensor research (Sekretaryova et al., 2014; Slaughter and Kulkarni, 2016; Sode et al., 2016). This is the first time a biosensor is incorporated inside a non-biological fuel cell.

In order to achieve the proposed goal, several steps were performed: catalyst modification with the ionomer and its influence on fuel cell performance (a sluggish reduction on fuel cell performance may hinder any practical application) and finally biosensor response evaluation.

2. Experimental section

2.1. Modification of the catalyst and preparation of the biosensor

PtRu (30:15 wt%)/carbon black (XC-72R) catalyst (or only carbon black XC-72R) was suspended at 1 mg/mL in a 2-(N-morpholino) ethanesulfonic acid (MES) solution (pH 5.5). Carbon black catalyst support is used as the initiator of the free radical co-polymerization of styrene, sulfonated styrene and and divinylbenzene (crosslinker) at concentrations of 0.375 mM, 0.225 mM and 0.30 mM respectively, in buffer, at T = 25 °C during 12 h. The target equivalent weight of the proton exchange capacity of the grafted polymer is 530 g/mol. For creating the binding cavities for the model target protein, a ferritin solution (final concentration 100 μg/mL) was previously mixed with aminoethyl methacrylate (for charge compensation, final concentration 1.1 μM) and added to the 1 mg/mL catalyst suspension in buffer (during 1 h). This allows protein adsorption on carbon black surface prior to polymerization initiation. After polymerization, protein template was removed by pH quenching in 0.5 M H_2SO_4, during 1 h, after polymerization. The modified catalysts were obtained by centrifugation, and washed 2 times with water and once with ethanol. The solids were dried in an oven at T = 60 °C during 48 h for further analysis while supernatant was immediately analysed by UV–vis. For the detailed list of reactants and materials used see the Supplementary information.

2.2. Characterization of the modified catalysts and biosensor response

Different techniques were used: a) Thermogravimetric experiments were conducted in platinum crucibles in an inert atmosphere (nitrogen, 100 mL min^{-1}, heating rate 20 °C/min); b) UV–visible spectroscopy (UV–vis) was used for tracking monomer polymerization. The absorption spectra of the sample is probed in the range of UV light, with a 2 nm bandwidth and 200 nm/min scan speed, relative to an appropriate reference control. A baseline is always previously acquired; c) Transmission electron microscopy images with different magnifications were acquired at 80 kV of accelerating voltage.

Regarding electrochemical characterization: a) The modified catalysts were re-suspended in isopropanol with 20 wt% Nafion in relation to the total catalyst mass and drop cast in carbon paper (gas diffusion layer) for preparing the catalytic layer of the electrode. Aiming proper electrode electrochemical cleaning and further ferritin iron core reduction (Marken et al., 2002) (in the event that any still remains in the cavities of the MIP modified catalyst), cyclic voltammetry was performed on 0.5 M H_2SO_4. The electrode was further characterized for methanol oxidation reaction (MOR) using 10 mM methanol in 0.05 M K_2SO_4 as electrolyte, platinum as counter electrode and Ag/AgCl as reference electrode at a sweep rate of 2.5 mV/s in linear sweep voltammetry (LSV); b) Direct methanol fuel cell: The anode with the catalytic layer for DMFC experiments was prepared and cleaned as described above, inserted in a suitable MEA and assembled in a single commercial cell (Pragma Industries – 5 cm^2) (as proof-of-concept an active fuel cell operation was considered in this work). The following operating conditions were used for obtaining the polarization curves (from open circuit potential down to 50 mV, 20 s polarization per point) and EIS (electrochemical impedance spectroscopy) analysis at

0.2 V: room temperature, atmospheric pressure, membrane: Nafion® 115, anode feed: 1 M methanol (1 mL min^{-1} (using a peristaltic pump), anode area: 2.2 cm^2; cathode feed: 100 mL min^{-1} of reconstituted air, a commercial cathode is used (0.5 mg_{Pt} cm^{-2} (2.2 cm^2); c) Rebinding of the target analyte was performed in a 3-electrodes configuration system using methanol as probe, and under DMFC environment (2-electrodes configuration). Ferritin was spiked in buffer solutions at different concentrations and each solution incubated on the electrode surface for 30 min. After each incubation step, the electrode was washed and characterized for methanol oxidation reaction (MOR), as described above (LSV). Rebinding in DMFC environment was also performed with consecutively increasing concentrations of protein further incubated at the anode side of the fuel cell. For that, DMFC performance is characterized (polarization curves and EIS), the fuel solution is then removed from the flow-field channels of the single cell unit and the spiked protein buffer solution is introduced. After the rebinding period (30 min), the protein solution is withdrawn and the anode is flushed with water. Fuel solution is reintroduced with help of the peristaltic pump and performance evaluated. These steps are repeated for the several protein concentrations to be tested. DMFC operating conditions are the same as above. For the selectivity measurements the same incubation procedure was followed, except that ferritin was spiked in a buffered solution of foetal bovine serum diluted 100× in the MES buffer.

All experiments were performed at least in duplicate. A control material (non-imprinted polymer (NIP)) is used in all the rebinding experiments; the same procedure as for plastic antibody synthesis is considered, however in the NIP material the protein adsorption step is eliminated prior to polymerization. All fuel cell performance tests are normalized by total catalyst mass (PtRu/C + polymer) for the modified materials and PtRu/C for the unmodified catalyst.

3. Results and discussion

This section addresses the following studies for biosensor development:

- Anchoring of the ionomer on the anode catalyst surface. A radically new and simple method is considered by using a one-step *grafting from* approach through radical polymerization which is triggered by the catalyst support. Carbon black is shown to quickly initiate polymerization of vinyl based monomers in aqueous media;
- Evaluation of the ionomer layer impact on fuel cell performance. The strategy used for molecular imprinting allowed the development of a completely new approach to the TPB of a fuel cell. Grafting a polymer with proton conductivity characteristics (an ionomer) allowed an increase on the triple phase contacts in the anode catalytic layer and an improvement on fuel cell performance;
- Rebinding characteristics of the biosensor. The response and selectivity of the biorecognition layer attached to the fuel cell catalyst was tested both in 3-electrodes configuration and DMFC environment. A clear and selective response from the biosensor was observed.

3.1. Anchoring of the ionomer on the anode catalyst surface

Ionomer *grafting from* carbon black surface followed a quite traditional methodology on MIP-based processes: surface imprinting through free radical polymerization. For that, the anchoring surface (in this case the catalyst) could be modified with a vinyl-based monomer. In this case, a carbonyl group activation process (Rebelo et al., 2014) covalently bonds the naturally occurring acidic functionalities (–COOH) on carbon surface to a vinyl-based monomer with a primary amine moiety. Following, a redox free radical polymerization of the vinyl-based monomers could be easily initiated by a redox pair (usually a peroxide/amine pair) (Braun, 2009) thus allowing low temperature and aqueous environment polymerization. These are critical conditions for having the protein is their natural conformation, a basic requirement for good mould imprinting of a protein.

However, with such redox initiation process, solution polymerization also competes with the surface imprinting process, undermining proper control of polymer thickness based on monomers´ concentration. This process despite quite simple imposes a harder control on the polymeric layer thickness during surface imprinting. Controlling thickness is important because under hydrated conditions, the polymer shell should not be thicker than ca. 5–8 nm, thus avoiding complete submersion of the protein on the polymer network, impeding selective mould recovery. A promising alternative to free radical polymerization is atom transfer radical polymerization (ATRP) (Adali-Kaya et al., 2015; Wang et al., 2016), a living polymerization that would allow grafting of the polymer from a strategically selective modified surface, thus avoiding solution polymerization. However, this method is more complicated than free radical polymerization and operation at low temperatures and aqueous environment is even more challenging (Matyjaszewski and Tsarevsky, 2014).

It has been reported that carbon black has free radicals on its surface (Boehm, 1994; Pena et al., 2001) as well as that these same free radicals are not able to initiate solely radical polymerization of vinyl based monomers (Liu et al., 2003; Ohkita et al., 1975; Tsubokawa et al., 1988) because of a more than 3 days period of polymerization inhibition (Kraus et al., 1959). This work will show that indeed carbon black is able to quickly initiate radical polymerization of different vinyl

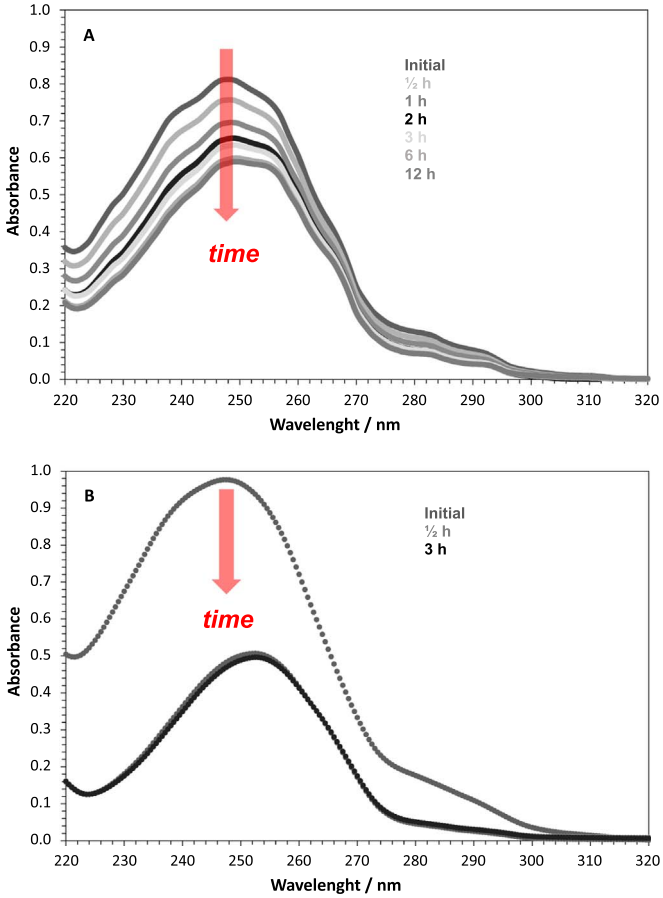

Fig. 1. (A and B) UV spectra of styrene based monomers in buffer solution during free radical polymerization initiated by: a peroxide/amine pair (1.0 mol.% of the initial monomers) – total polymerization time: 12 h (A), and carbon black (XC-72R) (B) – total polymerization time: 3 h. (C) Thermogram of a carbon black modified sample after 3 h radical polymerization of sulfonated styrene (0.225 mM, carbon black: 1 mg/mL in MES buffer). An unmodified carbon black sample dispersed in buffer (without monomer) and subjected to the same steps before analysis as the modified sample is also included. (D) TEM images of styrene-based monomers polymerized on: PtRu/XC-72R (left), XC-72R (top right) and unmodified carbon black (bottom right). Arrows show polymer-rich features.

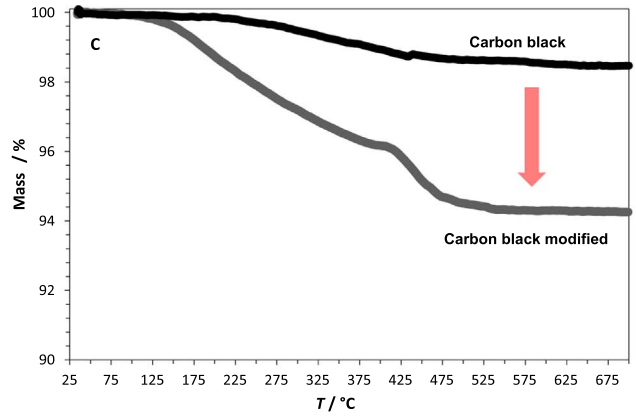

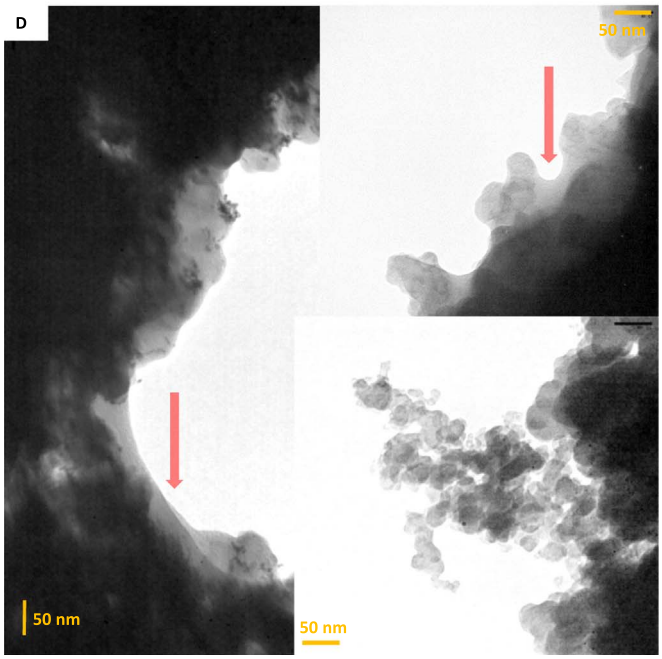

Fig. 1. (*continued*)

monomers under specific conditions thus avoiding solution polymerization and while using a quite simple procedure.

Styrene-based monomers undergoing radical polymerization were tracked by UV at 247 nm (Fig. 1(A)). The arrow points to the decrease in peak absorbance of those monomers (total initial concentration 0.9 mM) with polymerization time (total polymerization time 12 h, samples analysed every half an hour initially) after initiation by the peroxide/amine pair potassium persulfate/*N*,*N*,*N*',*N*'-Tetramethylethylenediamine (carbon black based catalyst absent). A control experiment without the initiator pair was also analysed by UV and no variation in absorbance was observed within the same experimental time scale (data not shown). In the presence of carbon black and absence of the initiator pair, Fig. 1(B) shows a quicker decrease on peak absorption (after ½ h reaction) for the same system; a nearly 50% monomer conversion was observed (according to Beer-Lambert law) (total polymerization time – 3 h). Supplementary information details the study followed by UV to track radical polymerization of the styrene-based monomers (Fig. S1).

These results point that the decrease on absorbance at ca. 250 nm in the absorption spectra is due to a decreased monomer concentration in the solution due to polymerization. Results also show that carbon black alone is capable of very quick initiation of polymerization (within 20 min). The success of polymerization initiation under these conditions may be related to the carbon black to monomer ratio. Radical polymerization of vinyl-based monomers in the presence of carbon black (for other types of applications) usually occurs in much higher monomer to carbon black ratios (usually monomer: carbon black 100: 1 mass ratio), and commonly using the monomer itself as the dispersant for carbon black during polymerization (bulk polymerization) (Tsubokawa, 1992). In our case, it is the opposite ratio, carbon black is in a much higher concentration than monomers (monomer: carbon black 1:4 mass ratio). This way the total amount of free radicals on carbon black surface can quickly trigger polymerization. The very thin layer of polymer that is required taking into account protein size allows the use of very low monomer concentrations. Reported strategies aiming polymeric modification of carbon black usually involve much higher thickness once the polymer is usually embedding the carbon black particles in their targeted applications (such as ink or tire industries) (Tsubokawa, 1992). Concluding, this method is much simpler than for instance ATRP and than using an initiator pair that would also allow solution polymerization.

Polymer grafting from carbon black surface, after ultra-pure water washing and drying of the resultant modified material, was analysed by thermogravimetry under inert environment. Fig. 1(C) shows one representative thermogram for both polymer-modified and unmodified carbon black materials. We can see that when polymer is present, a higher mass loss after 200 °C is observed due to the thermal decomposition of the polymer in comparison to the non-modified carbon black (control). The mass loss on the modified catalyst is ca. 4 wt% in accordance with the low monomer concentration on solution during polymerization and also because of the inert environment that probably is pyrolizing the grafted polymer instead of removing it (thermal analysis under oxidative conditions burns-off all the material, polymer and carbon black, being thus inconclusive). In conclusion, Fig. 1(C) shows that polymer modified carbon black becomes thermally less stable in comparison to the non-modified carbon black, as expected, due to the organic nature of the polymeric modification. Different types of monomers, concentrations and solvents were also tested showing clear changes in their thermograms due to polymer presence (data not shown).

Fig. 1(D) shows some TEM images obtained after the polymerization of styrene-based monomers performed in aqueous media in the presence of the carbon support and without any redox initiator pair. Polymerized products were also observed by TEM departing by other vinyl-based monomers such as acrylates and acrylamides in the presence of carbon black and without initiator (data not shown). It should be however emphasized that under such analysis conditions polymer is dehydrated and can be easily damaged by the high voltages usually applied. Additionally, the very thin layer (ca. 5 nm in hydrated conditions) shell and non-contrasting property of polymers in TEM analysis makes it even more difficult to be observed by this technique. Even though, the presence of the polymer is clearly evident in some spots and carbon support is completely embedded by the polymer. As comparison, Fig. 1(D) (bottom right) shows the morphology of unmodified carbon black.

The capacity of other allotropic forms of carbon, in aqueous environment, as well as that of carbon black, in organic solvents, to initiate radical polymerization was also observed. This approach introduces a highly simple method for allotropic carbon modification and opens the doors for an easier and simple surface modification, paving ways for nanotechnology, polymer science and other research field's development.

After the preliminary set of studies related to the anchoring of the polymeric layer on catalyst surface (see above), we are now able to consider such polymerization conditions for plastic antibody development – the MIP based biorecognition element of the biosensor. Fig. 2 sketches the steps involved on plastic antibody development, departing from a suspension of catalyst (a). In the first step, protein is adsorbed on the catalyst surface in a buffered solution (the model protein ferritin was chosen owing to its iron core easily observable by TEM, besides its isoelectric point, 3D structure and size are well-known) (b). Following, a suitable monomer formulation is added to the catalyst suspension and polymerization is let to occur (c). Finally, protein is removed by pH quenching in acidic solution for protein denaturation, releasing the cavities for further rebinding (d).

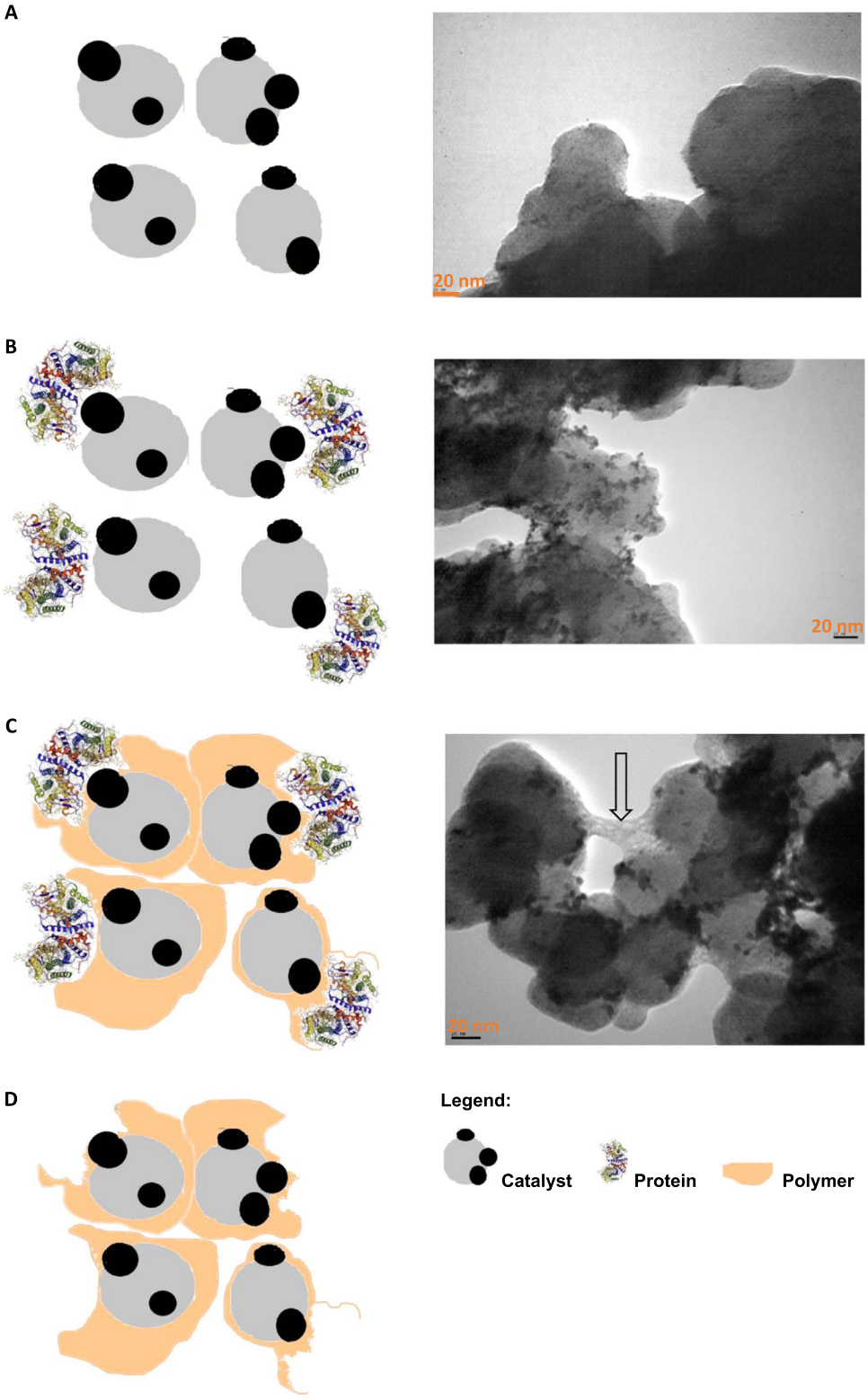

Fig. 2. Sketch of biosensor assembling by free radical polymerization. TEM images during assembling when possible. (a) PtRu/CB catalyst, (b) adsorption of ferritin (model protein), (c) polymerization step (evidencing a polymeric bridge formation), (d) removal of the template.

3.2. Evaluation of the polymeric layer impact on MOR and DMFC performance of the PtRu/C modified anode catalysts

A special concern when adding a polymer shell around the catalyst particles is its effect on methanol electrochemical activity. MOR activity could decrease and if fuel cell efficiency is too low this could bring a problem to the development of a small, cheap, autonomous biosensor device compactly integrated inside the DMFC. For an electrically autonomous biosensor operation, the catalytic activity of the fuel cell where the biosensor is inserted should be sufficient to power the signalling device.

MOR performed in K_2SO_4 electrolyte was used to further characterize the different modified electrocatalysts. Fig. 3(A) shows methanol oxidation in the 3-electrodes configuration system, evidencing that

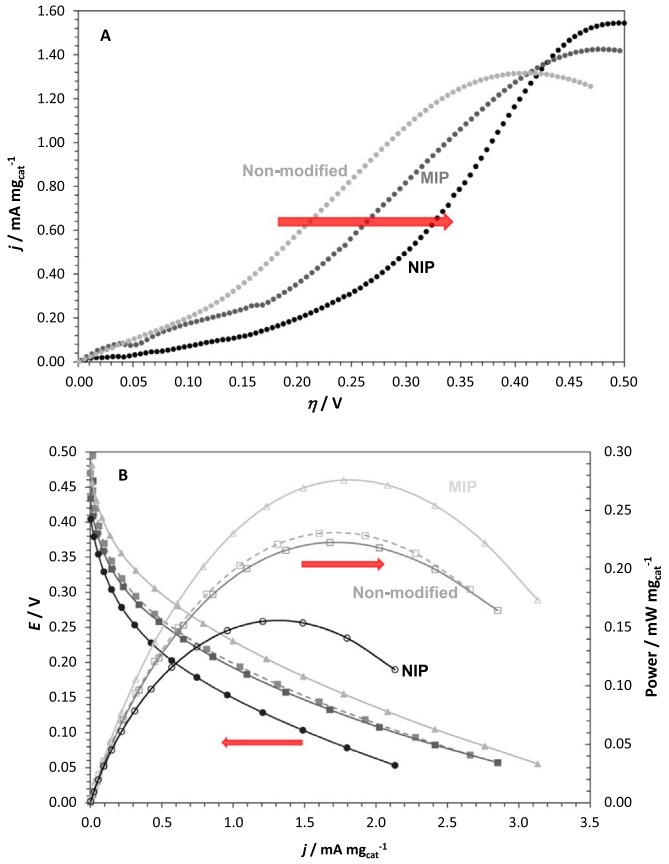

Fig. 3. (A) Methanol oxidation reaction in three electrodes configuration system. Sweep rate: 2.5 mV/s, electrolyte: 10 mM methanol in K_2SO_4 0.05 M. (B) DMFC performance of different anode catalysts: (Δ, ▲) molecular imprinted modified (MIP); (○, •) non-imprinted modified (NIP) and (□, ■) control (non-modified) (two independent control electrodes are included (dash line), reproducibility awareness is similar in the other cases). Open symbols: power curves, closed symbols: I/V curves.

MOR is hindered by the presence of the polymer. MOR overpotential for both modified materials is higher (standard potential considered was the curve interception with the horizontal axis (i = 0 A) in the voltammogram) than the non-modified catalyst. The non-imprinted polymer (NIP), used as control, shows higher overpotentials than the imprinted polymeric layer. In the later, the presence of the selective cavities allows a direct methanol access to the catalytic active sites decreasing overpotential. It should also be pointed out that the mass transport limitation regions seem to be not highly affected by the presence of the polymer (Cottrell region).

A commercial single cell was used for evaluating fuel cell performance of the modified anode catalysts and compared to that when an unmodified catalyst is used. Polarization curves as function of the mass specific current are plotted on Fig. 3(B). The non-imprinted polymer affected negatively fuel cell performance when compared to the non-modified catalyst, while the imprinted polymer affected performance positively (ca. 30% increase in peak power density). A similar molecular level approach to the triple phase boundary has been applied before for the cathode side of a H_2/O_2 fuel cell (Dru et al., 2016).

The increase in performance is related to polymer composition: by one side, a proton conductor polymer formulation (ionomer) was idealized for the specific application in a proton exchange membrane fuel cell. The polymer composition is based on a proton acceptor monomer (sulfonated styrene), a non-charged hydrophobic monomer (styrene) and a crosslinker (divinylbenzene) (target EW: ca. 500). The proton conductor polymer assembled on the surface of the catalyst probably improves TPB (pore/proton conductor/electron conductor triple intersection) sites inside fuel cell anode due to its high exchange capacity (ca. twice in comparison to the most used form of Nafion (EW = 1100)), which is a critical parameter in fuel cell performance. Nevertheless, further studies are undergoing in order to infer the final polymer composition; different monomer reactivity under free radical polymerization may occur despite the similar moieties (styrene derivatives)).

On the other side, cavities created on the plastic antibody due to protein presence (acting as macroporogen) allow a quicker access of methanol to the surface. At the cavities´ catalyst surface perimeter, the grafted ionomer then quick and selectively drives the protons produced at the near metal active sites to the Nafion membrane that separates both electrodes. Because of this, fuel cell performance improves. On the other hand, at the non-imprinted modified anode catalyst there are no cavities. This way, the TPB is indeed negatively affected by the polymer presence that hinders the access of methanol to the catalyst surface. It should be emphasized that ionomer covalent binding occurs through the carbon surface, thus minimally affecting catalytic metal sites that remain ideally free. A molecular level approach to the TPB by *grafting* proton conducting polymers *from* the carbon surface has never been addressed. A much more substantial impact on the cathode side of a PEMFC fuel cell is expected with such molecular level modification of TPB owing to the lower water content in the electrode which penalizes proton transport in comparison to the DMFC anode (Dru et al., 2016; Ferrandez et al., 2013). However, metal catalyst utilization and the effectiveness factor of catalyst utilization (O'Hayre et al., 2005; Uchida et al., 2013) are not the aim of the present work.

3.3. Characterization of the biosensor during rebinding

Rebinding characterization was performed initially in a 3-electrodes configuration system, using methanol oxidation reaction, as the sensor response. Fig. 4 shows the rebinding of the target protein (ferritin) on the MIP- and NIP-modified catalysts (CB/PtRu). A reverse trend between methanol oxidation peak current and protein concentration is observed for the MIP modified material while the NIP catalyst material shows a random response against concentration, indicating that the protein rebinds to the surface cavities of the MIP material. Lower and higher concentrations than the ones presented were tested but no differences in MOR were observed beyond concentration limits herein presented. The calibration equation for the MIP material in the 3-electrodes configuration system is presented in the insert of Fig. 4(A). A linear response with a negative slope is observed for methanol oxidation peak current as function of the logarithm of ferritin concentration.

Fig. 5(A and B) shows the response of the developed plastic antibody and its control (NIP) to known ferritin concentrations, in the DMFC environment (here a different Gas Diffusion Layer was used - with a microporous layer; this decreased power performance in comparison to that presented on Fig. 3(B) (untreated Toray paper), however performance became similar to a commercial electrode – Supporting information, Fig. S2). Fig. 5(A) shows a clear change in the power curve with ferritin (target protein) concentration for the plastic antibody modified anode. DMFC performance increases with ferritin concentration. This could be related to some proton conductivity capacity of the protein molecule when rebinding to the cavity, however further understating needs to be addressed. The calibration equation for the MIP material inside the fuel cell is presented in the insert of Fig. 5(A). A linear response with positive slope is observed for the peak power density as function of the logarithm of ferritin concentration.

Fig. 5(A) shows that plastic antibody responds to ferritin concentrations from 0.02 pM (10 pg/mL- 3 orders of magnitude lower than the common physiological range e.g. for some cancer markers (Vachani, 2016)) up to 20 pM, after which reached saturation (2 orders of magnitude higher concentration was tested and confirmed saturation). Additionally, the concentration detection limit has decreased ca. 2 orders of magnitude in comparison to the characterization performed in the 3-electrodes configuration system. This points to the advantage

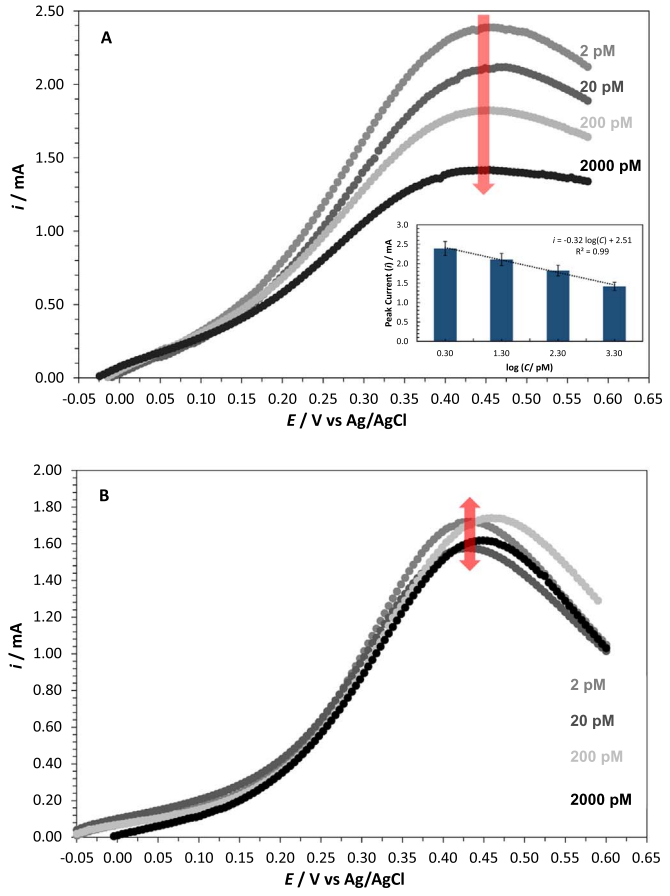

Fig. 4. Methanol electroxidation response to different buffered ferritin concentrations (probe: 10 mM methanol in 0.05 M K_2SO_4, sweep rate: 2.5 mV/s): (A) Plastic antibody (MIP). Inset: Methanol oxidation peak as function of the logarithm of protein concentration; (B) non-imprinted (NIP).

of using the biosensor under the fuel cell operation mode and not in a 3-electrodes configuration system. This last configuration could be feasible when using e.g. an external printed small battery and by adding proper control electronics; however, this increases both costs of the device and detection concentration limits. The decrease of the detection limit can be related to the absence of ionic species in the fuel solution feeding the fuel cell. Contrarily, in the 3-electrodes system, the ionic species from the electrolyte could displace some of the protein molecules from the cavities. Controversially, the higher concentration sensitivity limit decreased in the 2-electrodes system; this may be related to the pressing of the MEA inside the single cell (2.5 MPa) that could have collapsed some of the rebinding sites. Undergoing studies are being performed to find a compromise between fuel cell performance and biosensor sensitivity range. Current work is also focused on the development of a suitable passive DMFC design, scale-down, as well as the corresponding operating conditions and MEA assembling for introducing the plastic antibody.

Fig. 5(B) shows the same procedure performed on the (control) non-imprinted modified anode (NIP) where only a random, actually a nearly steady response can be observed. Fig. 5(B) also shows that NIP-modified catalytic fuel cell performance in lower than its MIP counterpart, in accordance with Fig. 3(B). Finally, the representative effect of the MES buffer on DMFC performance prior to protein solution incubation can be seen in Supplementary information (Fig. S3) (blank drift). Successive four blank buffer incubations incurred in a relative standard deviation from the averaged blank response lower than 1% (data not shown), thus indicating the high stability of the present system.

Electrochemical impedance spectroscopy (EIS) was also used to track biosensor response; anode charge transfer resistance decreased with analyte concentration in accordance with the power curves (please see Fig. S5, in the Supporting information). However, the use of EIS is out of the scope of the present work because this technique requires powerful equipment and technical skills, not proper for an easy, low-cost, user-friendly routine health care application.

The response of the biosensor in contact with biological fluids in DMFC environment was also considered. Foetal bovine serum was used as a simple biological fluid that can mimic human fluids and helps understanding the effect on those fluids on fuel cell performance. For that, serum was diluted in buffer and spiked with different concentrations of ferritin. A control experiment was also performed with the non-imprinted modified anode catalyst (NIP).

Fig. 5(C) shows that DMFC performance increases with ferritin spiked concentration in diluted bovine serum, and in accordance with Fig. 5(A), for the plastic antibody. The calibration equation for the selectivity experiments of the MIP material inside the fuel cell is presented in the insert and a linear response with a positive slope is observed for the peak power density as function of the logarithm of ferritin concentration. Fig. 5(D) shows the response on the control (NIP) electrode to the same range of concentrations as in Fig. 5(A), in DMFC environment. In this case, control showed a random response to ferritin spiked concentrations, in accordance with previous observations. Moreover, Fig. 5(C and D) also shows that DMFC performance is not affected by the serum fluids when they are diluted in the buffer used (please compare with DMFC performance, Fig. 3(A and B)) thus performance changes resulting from the simple exposure to the analyte sample are minimized. However, sample dilution is indeed required for biosensor stability; see Supporting information for further details on this issue.

Current work is undergoing for studying the application of this technology to cancer biomarkers allowing early cancer screening in collaboration with the Portuguese Institute of Oncology – Porto. One of the goals of such screening test is to diagnose cancer in different stages of disease. The advantage of the herein proposed biosensor is that it can become really cheap (however its current cost depends on ca. 90% to the high expensive antigens used) thus can be thoroughly used routinely for cancer screening.

4. Conclusions

The development of an electrical biosensor with potential to be fully autonomous (non-implantable), very small, and disposable due to the low cost (human resources and equipment are usually the most expensive ones) is proposed by an innovative approach to the biosensor transducer. This new device may bring possible relevant screening of several disease markers everywhere even in low income countries (e.g. for tuberculosis). The systematic application for e.g. cancer relapse screening in routine health services can also be achieved. The relevant disease markers to be considered are under evaluation with health-related researchers and taking into consideration Health Systems regulatory laws and respective priorities.

In this work, carbon black supporting catalysts were demonstrated for the first time to be capable solely of a very quick initiation of the radical polymerization of vinyl based monomers in aqueous media. Moreover, molecular imprinting allowed the design of a completely new approach to the TPB of the fuel cell. The biorecognition layer grafted with proton conductivity characteristics allowed a uniform distribution of triple phase contacts at the anode catalyst layer, which proved to actually increase fuel cell performance in comparison to the non-modified material catalytic performance. Finally, the response and selectivity of the biorecognition layer inserted in the anode of the fuel cell was demonstrated in DMFC environment for a model protein.

This work aims to be a demonstration of the concept herein proposed, not aiming a biosensor for ferritin neither presenting a final solution for this approach. But showing instead that the concept is

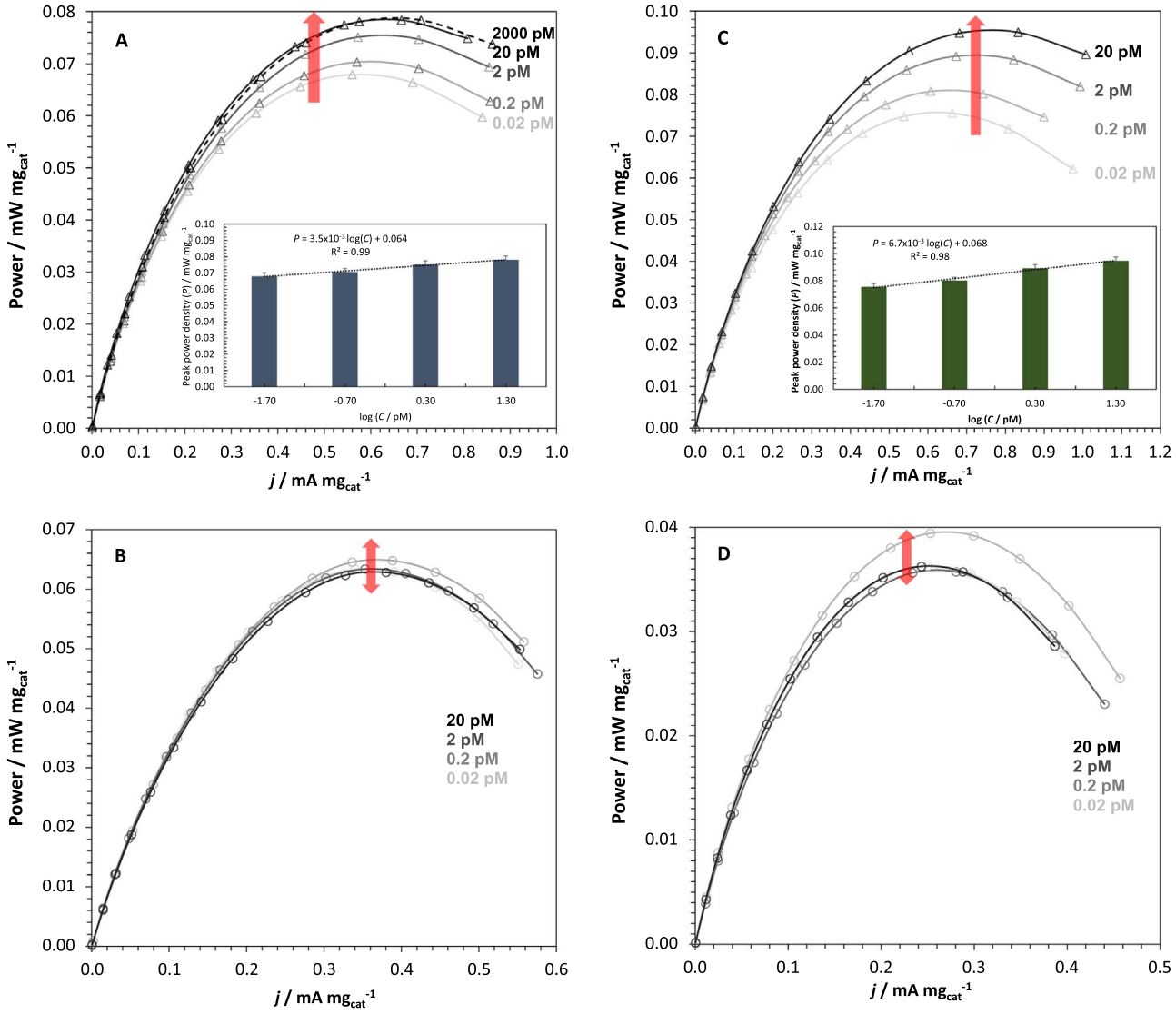

Fig. 5. (A and B) DMFC response to ferritin concentrations in buffer: (A) Plastic antibody (dashed line 2000 pM). Inset: Peak power mass density as function of the logarithm of protein concentration; (B) Control (NIP). (C and D) DMFC response to the target protein concentration spiked in foetal bovine serum (diluted 100× in buffer): (C) Plastic antibody. Inset: Peak power mass density as function of the logarithm of protein concentration; (D) Control (NIP).

possible, even though substantial amount of work still needs to be done in order to achieve a reliable, cheap, user-friendly, passive fuel cell operating, health-related screening device. The proposed methodology also brings importance to the interdisciplinary approach to science.

Note

A patent pending process is related to this work (Nr: 109856, INPI).

Acknowledgments

L. Brandão (coordinator of the Symbiotic project) and G. Sales (coordinator of BioMark) thank the financial support to the European Commission through the Horizon 2020 program, Pillar of Excellence (Future and Emerging Technologies – OPEN) with Grant agreement no. 665046 (2015) (http://symbiotic-project.eu/).

Appendix A. Supporting information

Supplementary data associated with this article can be found in the online version at doi:10.1016/j.bios.2017.07.021.

References

Adali-Kaya, Z., Bui, B.T.S., Falcimaigne-Cordin, A., Haupt, K., 2015. Molecularly imprinted polymer nanomaterials and nanocomposites: atom-transfer radical polymerization with acidic monomers. Angew. Chem.-Int. Ed. 54 (17), 5192–5195.

Asghary, M., Raoof, J.B., Rahimnejad, M., Ojani, R., 2016. A novel self-powered and sensitive label-free DNA biosensor in microbial fuel cell. Biosens. Bioelectron. 82, 173–176.

Boehm, H.P., 1994. Some aspects of the surface-chemistry of carbon-blacks and other carbons. Carbon 32 (5), 759–769.

Braun, D., 2009. Origins and development of initiation of free radical polymerization processes. Int. J. Polym. Sci..

Cardoso, A.R., Moreira, F.T.C., Fernandes, R., Sales, M.G.F., 2016. Novel and simple electrochemical biosensor monitoring attomolar levels of miRNA-155 in breast cancer. Biosens. Bioelectron. 80, 621–630.

Dru, D., Baranton, S., Bigarre, J., Buvat, P., Coutanceau, C., 2016. Fluorine-free Pt nanocomposites for three-phase interfaces in fuel cell electrodes. ACS Catal. 6, 6993–7001.

Ferrandez, A.C., Baranton, S., Bigarre, J., Buvat, P., Coutanceau, C., 2013. Chemical functionalization of carbon supported metal nanoparticles by ionic conductive polymer via the "grafting from" method. Chem. Mater. 25 (19), 3797–3807.

Han, Y.J., Chabu, J.M., Hu, S.Q., Deng, L., Liu, Y.N., Guo, S.J., 2015. Rational tuning of the electrocatalytic nanobiointerface for a "Turn-Off" biofuel-cell-based self-powered biosensor for p53 protein. Chem.-Eur. J. 21 (37), 13045–13051.

Kim, M., Hyun, M.S., Gadd, G.M., Kim, H.J., 2007. A novel biomonitoring system using microbial fuel cells. J. Environ. Monit. 9 (12), 1323–1328.

Kraus, G., Gruver, J.T., Rollman, K.W., 1959. The effects of carbon blacks on the free radical thermal polymerization of styrene. In: Zhou, Y. (Ed.), Carbon: Proceedings of the Fourth Conference, University of Buffalo.

Liu, T.Q., Jia, S., Kowalewski, T., Matyjaszewski, K., Casado-Portilla, R., Belmont, J., 2003. Grafting poly(n-butyl acrylate) from a functionalized carbon black surface by atom transfer radical polymerization. Langmuir 19 (16), 6342–6345.
Marken, F., Patel, D., Madden, C.E., Millward, R.C., Fletcher, S., 2002. The direct electrochemistry of ferritin compared with the direct electrochemistry of nanoparticulate hydrous ferric oxide. New J. Chem. 26 (2), 259–263.
Mathur, A., Blais, S., Goparaju, C.M.V., Neubert, T., Pass, H., Levon, K., 2013. Development of a biosensor for detection of pleural mesothelioma cancer biomarker using surface imprinting. PLoS One 8 (3), 8.
Matyjaszewski, K., Tsarevsky, N.V., 2014. Macromolecular engineering by atom transfer radical polymerization. J. Am. Chem. Soc. 136 (18), 6513–6533.
Moreira, F.T.C., Sale, M.G.F., Di Lorenzo, M., 2017. Towards timely Alzheimer diagnosis: a self-powered amperometric biosensor for the neurotransmitter acetylcholine. Biosens. Bioelectron. 87, 607–614.
O'Hayre, R., Barnett, D.M., Prinz, F.B., 2005. The triple phase boundary – a mathematical model and experimental investigations for fuel cells. J. Electrochem. Soc. 152 (2), A439–A444.
Ohkita, K., Tsubokawa, N., Saitoh, E., Noda, M., Takashina, N., 1975. FREE-radical polymerization of vinyl monomers in presence of. Carbon-Black Carbon 13 (5), 443–448.
Pena, J.M., Allen, N.S., Edge, M., Liauw, C.M., Hoon, S.R., Valange, B., Cherry, R.I., 2001. Analysis of radical content on carbon black pigments by electron spin resonance: influence of functionality, thermal treatment and adsorption of acidic and basic probes. Polym. Degrad. Stab. 71 (1), 153–170.
Rebelo, T., Pereira, C.M., Sales, M.G.F., Noronha, J.P., Costa-Rodrigues, J., Silva, F., Fernandes, M.H., 2014. Sarcosine oxidase composite screen-printed electrode for sarcosine determination in biological samples. Anal. Chim. Acta 850, 26–32.
Sadeghi, E., Putz, A., Eikerling, M., 2014. Effects of ionomer coverage on agglomerate effectiveness in catalyst layers of polymer electrolyte fuel cells. J. Solid State Electrochem. 18 (5), 1271–1279.
Sadik, O.A., Aluoch, A.O., Zhou, A.L., 2009. Status of biomolecular recognition using electrochemical techniques. Biosens. Bioelectron. 24 (9), 2749–2765.
Schirhagl, R., 2014. Bioapplications for molecularly imprinted polymers. Anal. Chem. 86 (1), 250–261.
Sekretaryova, A.N., Beni, V., Eriksson, M., Karyakin, A.A., Turner, A.P.F., Vagin, M.Y., 2014. Cholesterol self-powered biosensor. Anal. Chem. 86 (19), 9540–9547.
Slaughter, G., Kulkarni, T., 2016. A self-powered glucose biosensing system. Biosens. Bioelectron. 78, 45–50.
Sode, K., Yamazaki, T., Lee, I., Hanashi, T., Tsugawa, W., 2016. BioCapacitor: a novel principle for biosensors. Biosens. Bioelectron. 76, 20–28.
Tsubokawa, N., 1992. Functionalization of carbon-black by surface grafting of polymers. Progr. Polym. Sci. 17 (3), 417–470.
Tsubokawa, N., Fujiki, K., Sone, Y., 1988. Radical grafting from carbon-black - graft-polymerization of vinyl monomers initiated by peroxyester groups introduced onto carbon-black surface. Polym. J. 20 (3), 213–220.
Uchida, M., Park, Y.C., Kakinuma, K., Yano, H., Tryk, D.A., Kamino, T., Uchida, H., Watanabe, M., 2013. Effect of the state of distribution of supported Pt nanoparticles on effective Pt utilization in polymer electrolyte fuel cells. Phys. Chem. Chem. Phys. 15 (27), 11236–11247.
Vachani, C., 2016. In: Pennsylvania, T.A.C.C.o.t.U.o. (Ed.). ⟨https://www.oncolink.org/cancer-treatment/procedures-diagnostic-tests/blood-tests-tumor-diagnostic-tests/patient-guide-to-tumor-markers⟩.
Viswanathan, S., Rani, C., Ribeiro, S., Delerue-Matos, C., 2012. Molecular imprinted nanoelectrodes for ultra sensitive detection of ovarian cancer marker. Biosens. Bioelectron. 33 (1), 179–183.
Wang, H.S., Song, M., Hang, T.J., 2016. Functional interfaces constructed by controlled/living radical polymerization for analytical chemistry. ACS Appl. Mater. Interfaces 8 (5), 2881–2898.
Zahedi, P., Ziaee, M., Abdouss, M., Farazin, A., Mizaikoff, B., 2016. Biomacromolecule template-based molecularly imprinted polymers with an emphasis on their synthesis strategies: a review. Polym. Adv. Technol. 27 (9), 1124–1142.